ADVANCED INTELLIGENT SYSTEMS
Open Access
www.advintellsyst.com

iPRISM: Intelligent Predicting Response to Cancer Immunotherapy through Systematic Modeling

Yinchun Su, Siyuan Li, Qian Wang, Bingyue Pan, Jiyin Lai, Guangyou Wang, Junwei Han,* and Qingfei Kong**

Immunotherapy has revolutionized cancer treatment, but predicting patient response remains challenging. Herein, we present iPRISM (Intelligent Predicting Response to cancer Immunotherapy through Systematic Modeling), which is a novel network-based model that integrates multiomics data to predict immunotherapy outcomes. In this approach, iPRISM incorporates gene expression, biological functional network, tumor microenvironment characteristics, immune-related pathways, and clinical data to provide a comprehensive view of factors influencing immunotherapy efficacy. Using stepwise logistic regression, we identified key predictive features and validated iPRISM across multiple cohorts including melanoma, bladder cancer, non-small cell lung cancer, and stomach adenocarcinoma. We also find that iPRISM outperforms the existing methods, achieving high predictive accuracy and demonstrating significant prognostic value for overall and progression-free survival. By identifying key genetic and immunological factors, this model provides a new insight for more personalized treatment strategies and combination therapies to overcome resistance mechanisms. iPRISM can be accessed at CRAN: https://CRAN.R-project.org/package=iPRISM.

1. Introduction

The introduction of immunotherapy has revolutionized the landscape of cancer treatment, providing new hope for patients with advanced-stage cancers.[1] Immune checkpoint inhibitors are a type of immunotherapy, which have demonstrated remarkable efficacy in a subset of patients by harnessing the body's immune system to target and eliminate cancer cells.[2] However, despite these successes, the mechanisms underlying the lack of response or resistance to immunotherapies in some patients are complex and not fully understood.[3,4] This disparity highlights the pressing need for predictive models that can accurately identify patients most likely to benefit from immunotherapy by integrating various biological features, thereby optimizing treatment strategies and improving patient outcomes.[5]

The promise of immunotherapy lies in its ability to engage the immune system in the fight against cancer.[6] However, the complexity of immune interactions within the tumor microenvironment (TME) presents a significant challenge in predicting therapeutic outcomes.[7] Recent advancements in bioinformatics and systems biology have enabled the development of sophisticated models that integrate diverse biological data to decode the innate relationships between gene expression, immune pathways, and clinical responses. For instance, T helper 1 (Th1) and T helper 2 (Th2) cells play crucial roles in the immune responses against cancer development, with Th1 cells promoting cell-mediated immunity and Th2 cells stimulating the production of proinflammatory cytokines.[8,9] Enhanced T cell infiltration has been associated with improved responses to immunotherapy,[10] emphasizing the importance of infiltration of immune system in determining treatment efficacy.

In addition to T cell infiltration, several studies have identified genetic mutations that influence the effectiveness of immunotherapies across various cancers.[11,12] Somatic gene mutations can lead to resistance to T-cell-based immunotherapies by impairing the effector function of $CD8^+$ T cells, such as *APLNR* gene mutations.[13] High tumor mutation burden (TMB) has been associated with better overall survival (OS),

Y. Su, S. Li, Q. Wang, B. Pan, J. Lai, J. Han
College of Bioinformatics Science and Technology
Harbin Medical University
Harbin 150081, P. R. China
E-mail: hanjunwei@ems.hrbmu.edu.cn

The ORCID identification number(s) for the author(s) of this article can be found under https://doi.org/10.1002/aisy.202400717.

© 2024 The Author(s). Advanced Intelligent Systems published by Wiley-VCH GmbH. This is an open access article under the terms of the Creative Commons Attribution License, which permits use, distribution and reproduction in any medium, provided the original work is properly cited.

DOI: 10.1002/aisy.202400717

Y. Su, G. Wang, Q. Kong
Department of Neurobiology
Harbin Medical University
Harbin 150081, P. R. China
E-mail: wangguangyou@hrbmu.edu.cn; kqfangel@hrbmu.edu.cn

Q. Kong
The Heilongjiang Provincial Joint Laboratory of Basic Medicine and Multiple Organ System Diseases (International Cooperation)
Harbin, Heilongjiang 150086, P. R. China

Q. Kong
Department of Neurosurgery
The First Affiliated Hospital of Harbin Medical University
Harbin 150001, P. R. China

progression-free survival (PFS), and overall response rate (ORR) in diverse cancer patients receiving immunotherapy.[11,14–16] Specifically, in non-small cell lung cancer (NSCLC), higher nonsynonymous mutation burden correlates with improved response to PD-1 blockade therapy.[12] Mutations in genes such as *TP53*, *KRAS*, and *BRAF* are known to influence resistance or sensitivity to immune checkpoint inhibitors.[17,18] However, certain comutations, such as those involving *KEAP1*, *PBRM1*, *SMARCA4*, and *STK11*, can result in poor immunotherapy outcomes despite high TMB.[19] Therefore, profiling the genetic landscape of tumors is critical for predicting and optimizing immunotherapy responses.

Several computational models have been developed to predict prognosis and response to immunotherapy. The Tumor Immune Dysfunction and Exclusion (TIDE) model utilizes gene expression data to elucidate mechanisms of tumor immune evasion, offering insights into why certain tumors fail to respond to immune checkpoint blockade due to T cell dysfunction and exclusion.[20] Similarly, the immuno-oncology algorithm (IO score) predicts patient response to immunotherapies in NSCLC using gene expression data, providing independent and incremental predictive value over current biomarkers.[21] Another approach is the Modulator of TMB-Associated Immune Infiltration (MOTIF) model, which predicts immunotherapy response by analyzing transcriptome sequencing data, focusing on factors that regulate $CD8^+$ T cell infiltration and function.[22] However, these models are limited by their reliance on a single type of data, such as gene expression, without integrating the multifaceted aspects of the TME and genetic alterations.

To address these limitations of existing models, we propose Intelligent Predicting Response to cancer Immunotherapy through Systematic Modeling (iPRISM), a novel network-based prognosis prediction model that integrates multiple types of biological data to predict patient responses to immunotherapy. By incorporating gene expression data, biological functional network, TME characteristics, and immune-related pathways, the iPRISM model provides a comprehensive view of the factors influencing immunotherapy efficacy. The model utilizes advanced statistical methods, including stepwise logistic regression, to capture predictive features for therapeutic reaction. We have also validated the iPRISM model across multiple cancer types, including melanoma, bladder cancer (BLCA), NSCLC, and stomach adenocarcinoma (STAD), and evaluated its predictive accuracy and prognostic utility using independent testing cohorts. The performance of the iPRISM model has been compared with other established methods to demonstrate its superior predictive capabilities.

Furthermore, we explore the TME differences and mutation profiles between predicted responders and nonresponders to gain deeper insights into the biological mechanisms driving treatment outcomes. By integrating comprehensive biological data and advanced predictive modeling, the iPRISM model has the potential to significantly improve patient stratification for immunotherapy. This approach can enhance clinical outcomes by identifying patients most likely to benefit from immunotherapy while minimizing unnecessary side effects for nonresponders. Therefore, the iPRISM model will bridge the gap between the complexity of the TME and the clinical application of immunotherapy.

2. Experimental Section

2.1. Data Acquisition

To develop and validate the iPRISM model, we utilized a comprehensive datasets, Liu cohort,[23] which includes transcriptomic and clinical data from patients treated with immunotherapy. This cohort served as the primary data source for model development and training. For independent validation, we accessed two testing sets, PRJEB23709 and phs000452 which from the Tumor Immunotherapy Gene Expression Resource (TIGER) portal (link: http://tiger.canceromics.org/#/download). These testing sets provided transcriptomic data and clinical annotations for 91 and 153 clinical samples of patients receiving immunotherapy.[24,25]

Furthermore, we applied the iPRISM model to several additional datasets to evaluate its performance in specific cancer types. For BLCA, we used the IMvigor210 dataset that can be accessible through the IMvigor210CoreBiologies R package.[26] This dataset includes transcriptomic data and clinical information from patients with advanced urothelial carcinoma treated with the immune checkpoint inhibitor atezolizumab. In the case of NSCLC, we utilized GSE93157 dataset to explore the molecular mechanisms underlying treatment responses.[27] Similarly, for STAD, we employed the PRJEB25780 dataset from the TIGER portal for validation purposes,[28] which contains gene expression data but lacked clinical annotations. The dataset summary can be found in the Table S1, Supporting Information. The pathways used in the study were downloaded from Reactome database (Version 87, https://reactome.org/), which include 2,656 pathways.

2.2. Study Design of iPRISM

The iPRISM model employs a three-stage workflow, as illustrated in **Figure 1**: (1) identification of immune-related pathways, (2) identification of response-related pathways, and (3) application of the prediction model of immunotherapy response.

In the first stage, we identified immune-related pathways. Specifically, we collected three categories of immune-related genes: three immune checkpoint inhibitor (ICI) genes, 23 human leukocyte antigen (HLA) genes, and 141 TME genes (Table S2, Supporting Information). To ensure that our analysis captures the most immune-related pathways, we mapped three categories of gene sets onto a protein–protein interaction (PPI) network obtained from STRING (https://www.string-db.org/), respectively. Next, we applied the random walk with restart (RWR) algorithm to prioritize genes within the network. Using these ranked genes, we conducted Gene Set Enrichment Analysis (GSEA) to identify statistically significant immune-related pathways. The intersecting pathways with $p < 0.001$ across the three gene categories were selected for further analysis. This step obtained 31 significant pathways.

In the second stage, the identified immune-related pathways are coupled with patient-specific gene expression data to quantify

© 2024 The Author(s). Advanced Intelligent Systems published by Wiley-VCH GmbH

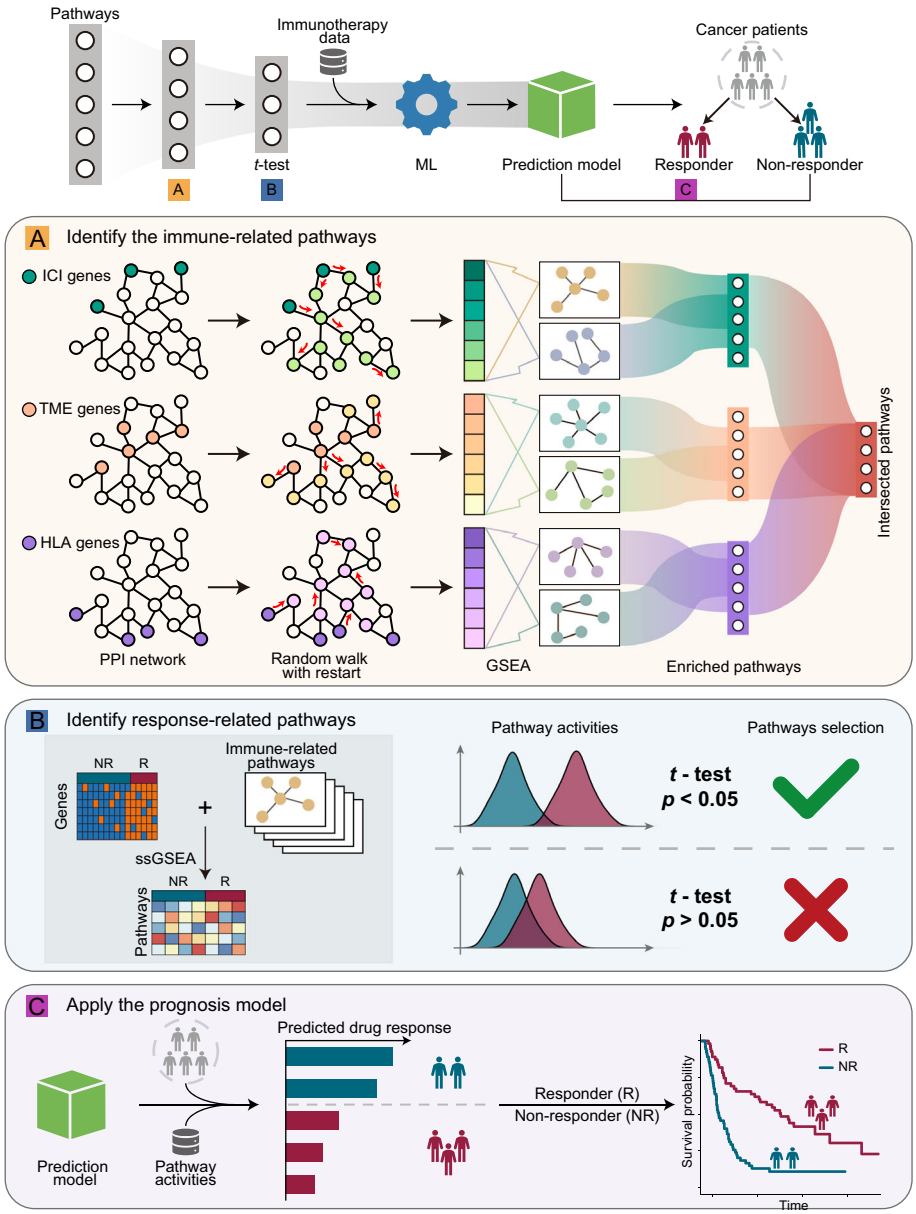

Figure 1. iPRISM workflow for predicting immunotherapy response. A) Schematic overview of the (iPRISM model. B) Detailed steps of the iPRISM model integrating critical biological networks. A) Identification of immune-related pathways. Integration of ICI, TME, and HLA genes into a PPI network. Application of RWR algorithm to prioritize immunotherapy response-relevant genes. GSEA to identify enriched pathways and select crucial immune response intersection pathways. B) Identification of response-related pathways. Quantification of pathway activities in individual patients using single-sample GSEA (ssGSEA). Pairwise logistic regression to identify pathways with significant activity differences between responders (R) and nonresponders (NR) (p-values <0.05). C) Application of prediction model. Estimation of patient responses based on pathway activities using pairwise logistic regression. Validation against clinical outcomes, demonstrated by Kaplan–Meier survival curves showing significant differences between responders and nonresponders. This workflow illustrates the methodological steps in constructing and validating the iPRISM model, emphasizing its integration of immune-related pathways, identification of response-related pathways, and application of a prognostic model for predicting immunotherapy outcomes.

pathway activities. Gene expression data are a key input for estimating the activities of these immune-related pathways in individual patients. To achieve this, we use single-sample Gene Set Enrichment Analysis (ssGSEA) to estimate pathway activities for each patient, which allows us to quantify the activity of each pathway based on the gene expression levels. We then performed the student's t test to compare pathway activities between responders and nonresponders. Pathways showing significant differences ($p < 0.05$) were considered response-related.

In final training stage, the selected response-related pathways were used to train the prediction model to predict immunotherapy response. We employed stepwise logistic regression to identify the most statistically significant pathways that differ from nonresponders and responders. This iterative method selects

© 2024 The Author(s). Advanced Intelligent Systems published by Wiley-VCH GmbH

significant predictors while excluding nonsignificant ones, ensuring that only the most statistically significant pathways that contribute to treatment response are included in the final model. Finally, we constructed the iPRISM model and extracted the most relevant pathways contributing to immunotherapy response.

2.3. Feature Extraction Using Stepwise Logistic Regression

To refine the set of pathways that contribute to the prediction of immunotherapy response, we employed stepwise logistic regression, a widely used feature selection technique in predictive modeling. This approach aims to identify and subset most relevant pathways while excluding those that do not significantly contribute to the prediction.

The process of stepwise logistic regression combines two techniques: forward selection and backward elimination. Forward selection initiates with no pathways and sequentially adds predictors based on their contribution to improving the model performance until no additional variables significantly enhance the model. Conversely, backward elimination begins with all pathways and iteratively removes the least significant ones until only statistically significant pathways remain.

This stepwise approach iteratively adds and removes pathways to identify the optimal set of pathways. At each step, the model evaluates whether including or removing a pathway improves its predictive performance, remaining those pathways with the highest predictive power. This process ensures the model remain the most important pathways while avoiding overfitting.

In iPRISM, we employ stepwise logistic regression to the pathway activity score profiles derived from gene expression data. Initially, the activity profiles of 31 immune-related pathways were included as input features. The stepwise logistic regression then iteratively refined the model by selecting pathways that showed the strongest association with treatment response while excluding those with minimal or no predictive values. By implementing this, we trained iPRISM and constructed its model as iPRISM score:

$$\text{iPRISM} = \sum_{i=1}^{k} c_i p_i \tag{1}$$

where c_i is the coefficient of pathway p_i, and k is the number of pathways constructed in the iPRISM model. The critical pathways influencing treatment outcomes are presented in Table S1, Supporting Information.

To validate the iPRISM model, we employed independent datasets and evaluated its performance by comparing predicted drug responses with actual clinical outcomes. We assessed the model's predictive accuracy using receiver operating characteristic (ROC) curves and area under the curve (AUC) values. Furthermore, we generated Kaplan–Meier survival curves to compare OS and PFS between predicted responders and nonresponders. This comprehensive validation approach enabled us to rigorously assess the model's ability to stratify patients and predict immunotherapy outcomes across various cancer types.

2.4. Immune Cell Infiltration Analysis

We employed xCell to quantify the extent of Th1 and Th2 cell infiltration in tumor samples. xCell is a gene signature-based method that estimates the abundance of various immune cell types from gene expression data.[29] This approach provided a robust assessment of the tumor immune microenvironment. We then performed comparative analyses of Th1 and Th2 cell infiltration levels between responders and nonresponders to investigate their roles in mediating immune responses to immunotherapy, which can gain valuable insight into the interplay between tumor biology and the immune system in the context of immunotherapy.

2.5. Mutation Profiling and Co-Occurrence Analysis

We performed mutation profiling to identify genetic alterations in responders and nonresponders. Using maftools package, we generated waterfall plots to visualize the distribution and frequency of mutations across the cohorts.[30] Additionally, to identify significant patterns of genetic interactions, we conducted an analysis of mutually exclusive and co-occurring mutations using Fisher's exact test. We focused on the top 10 genes exhibiting mutually exclusive or co-occurring mutations in responders and nonresponders. The significance of these interactions was visualized using color-coded p-values. Mutually exclusive mutations identified in this analysis may indicate alternative pathways driving tumorigenesis, suggesting distinct mechanisms of cancer development and progression in different patient subgroups. Conversely, co-occurring mutations potentially signify synergistic effects contributing to cancer progression, offering insights into the cooperative genetic alterations that may influence treatment outcomes.

2.6. Statistical Analysis

Statistical analyses were conducted using R. The chi-square test was used to examine the association between model predictions and actual drug responses. ROC curves and AUC values were calculated using the "pROC" package in R. Survival analysis was performed using the "survival" package, and Kaplan–Meier curves and log-rank test were performed using the "survminer" package.

3. Results

3.1. Analysis of Featured Pathways in iPRISM Model

In this section, we presented the featured pathways within the iPRISM model and their correlations within various immune cell types, demonstrating the alignment of learned features with prior knowledge. In this case, we trained iPRISM and constructed its model as iPRISM scores. After diving into the iPRISM model, we found several key pathways were correlated with immune cell types.

Figure 2 illustrates the correlations between the activities of key immune-related pathways and different immune cell types. Figure S1, Supporting Information provides a detailed analysis of the top three pathways exhibiting the highest degree of cellular

© 2024 The Author(s). Advanced Intelligent Systems published by Wiley-VCH GmbH

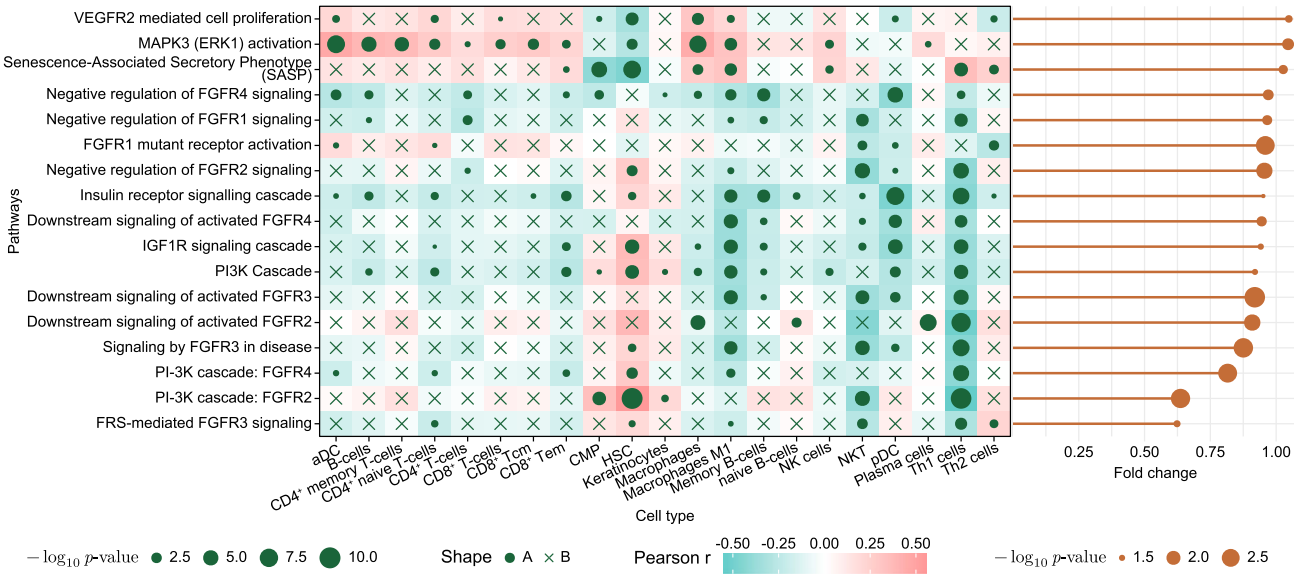

Figure 2. Correlation analysis of pathways and immune cells. The bubble plot in the left panel shows correlations between key immune-related pathways and immune cell types. Color intensity represents the Pearson correlation coefficient strength, while bubble size indicates statistical significance. The right panel displays the differential fold change of pathways between responders and nonresponders, highlighting pathways that significantly differentiate the two groups.

correlation with immune cells. Notably, pathways such as VEGFR2-mediated cell proliferation, MAPK3 activation, and senescence-associated secretory phenotype (SASP) show significant positive correlations with immune cells like macrophages ($R = 0.27$, $p = 0.0026$) and M1 macrophages ($R = 0.31$, $p = 4.6\text{e-}04$). These correlations suggest an enhancement of immune cell functions within the disease context.

In particular, the MAPK3 activation pathway demonstrated strong correlations with macrophages ($R = 0.45$, $p = 3.1\text{e-}07$) and M1 macrophages ($R = 0.32$, $p = 3.6\text{e-}04$), indicating its potential impact on immunotherapy outcomes (Figure S1, Supporting Information). Similarly, VEGFR2-mediated cell proliferation is associated with tumor angiogenesis. For patients with high activity in this pathway, antiangiogenic drugs such as Bevacizumab can be prescribed in combination with immunotherapy to reduce the formation of new blood vessels, limiting tumor growth, and improving immune infiltration into the tumor site. These findings align with previous studies that have highlighted the importance of VEGFR2 in angiogenesis and immune modulation,[31,32] and MAPK3 in cell proliferation and survival pathways.[33]

Conversely, the top three pathways showed negative correlations with specific immune cells, particularly hematopoietic stem cells (HSCs). For example, SASP showed a negative correlation with HSCs ($R = -0.46$, $p = 1.1\text{e-}07$, Figure S1, Supporting Information), indicating that high activity in this pathway might suppress HSC presence. This observation aligns with existing studies on the balance between stem cell quiescence and activation, emphasizing the importance of maintaining HSC quiescence for preserving regenerative capacity and preventing exhaustion and DNA damage.[34,35] Additionally, SASP has been shown to disrupt IL-1, which is crucial for HSC quiescence and maintenance.[36,37]

To further explore the relationships between iPRISM scores and immune cell infiltration, we examined the correlations between the iPRISM scores and various immune cell types, as shown in Figure S2, Supporting Information. Notably, we observed significant negative correlations with activated dendritic cells (aDCs), $CD4^+$ memory T cells, $CD4^+$ naive T cells, and $CD8^+$ T cells. This result suggests that higher iPRISM score may be associated with decreased immune cell populations. Additionally, we observed the same patterns with macrophages M1 and HSCs, which may suggest that the iPRISM model effectively captured these interactions between immune-related pathways and various immune cell types.

Moreover, we illustrated key pathways identified by iPRISM model. The final selected pathways are provided in Table S3, Supporting Information, along with a brief description of their known roles in immunotherapy and tumor-immune relationships in Supplementary Note 1, Supporting Information. It highlights the biological relevance of the pathways, which play critical roles in the immune response and tumor-immune interactions.

3.2. Prognostic Performance of iPRISM

We trained the iPRISM model using Liu cohort and subsequently evaluated its alignment with the actual immunotherapy response outcomes. Our analysis demonstrated that the iPRISM model effectively distinguished between responders (R) and nonresponders (NR) in the training set, confirming its capability to accurately identify patiented likely to benefit from immunotherapy. **Figure 3**A presents the results of a chi-square test comparing predicted responders and nonresponders to the actual drug response outcomes. The test yielded a highly significant result

© 2024 The Author(s). Advanced Intelligent Systems published by Wiley-VCH GmbH

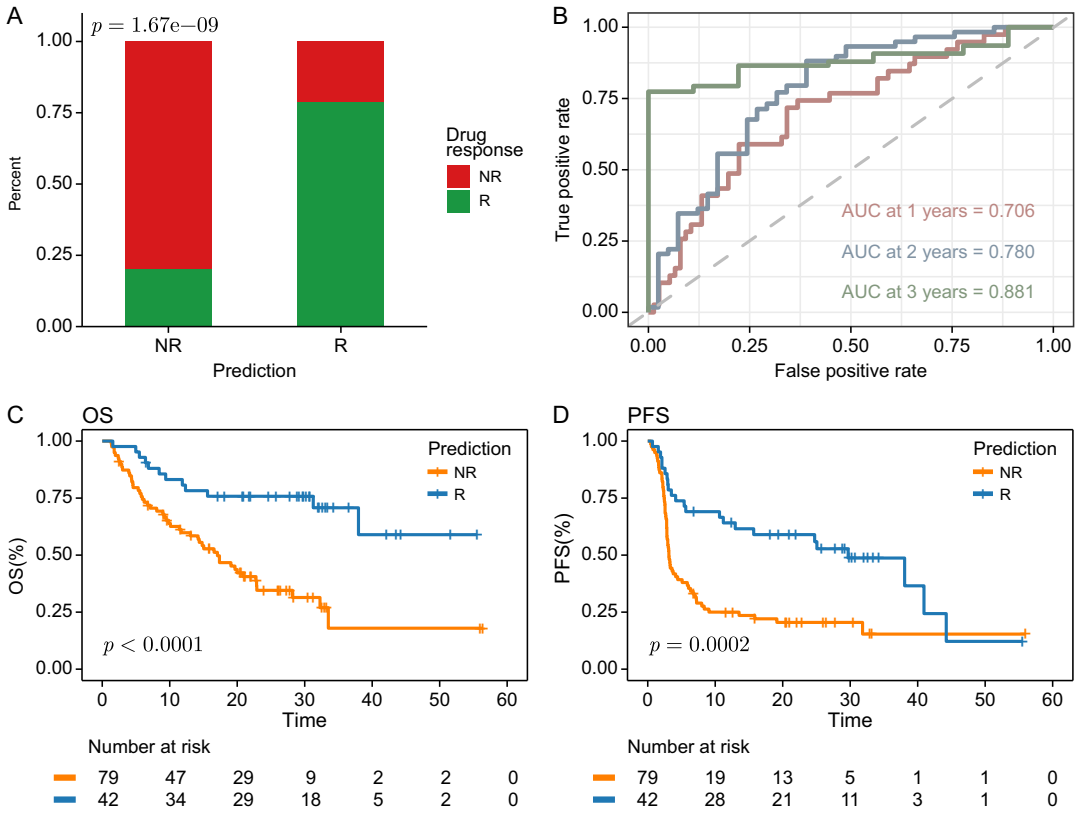

Figure 3. Prognostic performance of the iPRISM model in the training set. A) Chi-square test results showing the association between the model predictions and actual drug responses in the Liu cohort. Bar chart depicts the percentage of predicted responders and nonresponders. B) ROC curves illustrating the prediction accuracy of the iPRISM model at 1, 2, and 3 years. The AUC values indicate high predictive accuracy over time. C) Kaplan–Meier survival curves showing OS of patients predicted responders and nonresponders in the Liu cohort ($p < 0.0001$). D) Kaplan–Meier survival curves illustrating the PFS for the same patient groups, indicating a significant difference in PFS between responders and nonresponders ($p = 0.0002$).

($p = 1.67e-09$), indicating a strong association between the model's predictions and observed immunotherapy responses.

To illustrate the ability of the iPRISM model to distinguish between responders and nonresponders, we plotted the distribution of iPRISM scores for each group (Figure S3, Supporting Information). As shown, the iPRISM scores are significantly higher in responders compared to nonresponders ($p < 0.001$), demonstrating the model's discriminatory power.

To illustrate the performance over time, we presented the ROC curves for predictions at one-, two-, and three-years survival intervals. The AUC values at these time points were 0.706, 0.780, and 0.881, respectively. This indicates high predictive accuracy over time, with an improving trend suggesting enhanced performance in forecasting long-term outcomes.

We further examined survival outcomes based on the classification results of the iPRISM model.Figure 3C displays the OS of patients predicted to be responders versus nonresponders. The Kaplan–Meier survival curves revealed a significant difference in survival outcomes between the two groups ($p < 0.0001$), with responders exhibiting substantially better survival rates. This finding indicates that patients predicted to respond to treatment by the iPRISM model have a significantly improved OS. Similarly, Figure 3D illustrates the PFS for the same patient cohort. The Kaplan–Meier curves demonstrated a significant difference in PFS between responders and nonresponders ($p = 0.0002$). This result reinforces the model's ability to predict not only immediate drug response but also long-term clinical benefits.

3.3. Validation of the iPRISM Model on Independent Testing Sets

Having demonstrated sound validation results in predicting drug responses and survival outcomes using iPRISM in the Liu cohort, we further validated its performance using two separate melanoma testing sets. These independent immunotherapy datasets were used to assess the model's generalizability and robustness across different populations.

We first presented the ROC curves using two testing sets (**Figure 4**A). The ROC-AUC for both test cohorts exceeded 0.70, demonstrating strong predictive accuracy across diverse cohorts. To further evaluate the association between the model's predictions and actual immunotherapy responses, we performed chi-square tests as shown in Figure 4B. For both test cohorts, iPRISM achieved a significant correlation between predictions and actual responses, supporting the model's predictive validity.

© 2024 The Author(s). Advanced Intelligent Systems published by Wiley-VCH GmbH

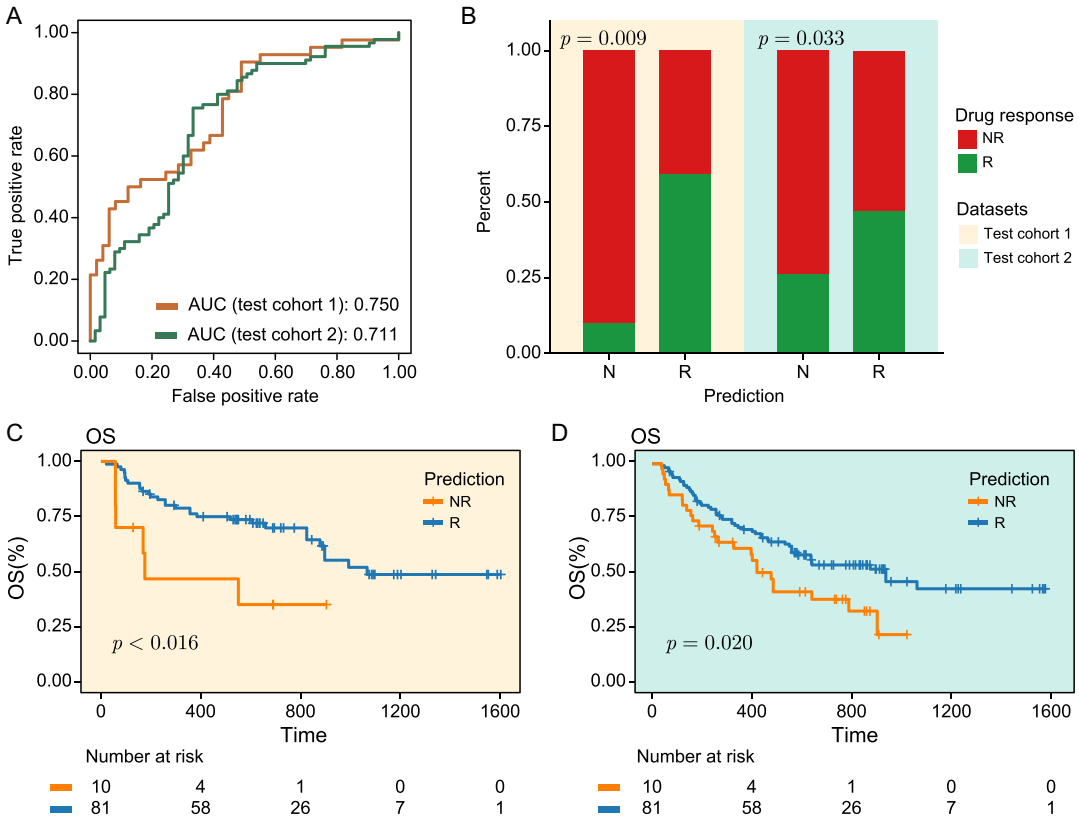

Figure 4. Validation of iPRISM on independent testing sets. A) ROC curves for the iPRISM model predictions in test cohort 1 (PRJEB23709) and test cohort 2 (phs000452). The AUC values demonstrate strong predictive accuracy across both datasets. B) Chi-square test results showing significant correlations between model predictions and actual drug responses in both testing cohorts. C) Kaplan–Meier survival curves for OS in test cohort 1, showing a significant difference between predicted responders and nonresponders ($p < 0.016$). D) Kaplan–Meier survival curves for OS in test cohort 2, indicating a significant difference between predicted responders and nonresponders ($p = 0.020$).

These results display the model's effectiveness in different cohorts, consistent with its performance in the training set.

We further conducted survival analysis to examine the prognostic significance of the iPRISM model in the independent testing sets. Figure 4C,D illustrate the OS outcomes based on the iPRISM-model's classification results. In test cohort 1 (Figure 4C), the Kaplan–Meier survival curves revealed a significant difference in OS between predicted responders and nonresponders ($p < 0.016$), with responders showing markedly better survival rates. Similarly, test cohort 2 in Figure 4D yielded a similar result, demonstrating a significant OS difference between predicted responders and nonresponders ($p = 0.020$). These consistent findings across both cohorts validate the model's utility in prognosticating patient outcomes and its potential for guiding personalized immunotherapy strategies.

3.4. Comparative Analysis of the iPRISM Model with Other Models

After demonstrating iPRISM captured relevant features of the prognosis and immunotherapy responses in melanoma using the Liu cohort and two independent testing sets, we further validated its performance by comparing it with 11 other established methods.

We first evaluated the predictive performance of iPRISM compared to other methods using Liu cohort. **Figure 5**A presents the ROC curves for all methods, with iPRISM demonstrating superior predictive performance as evidenced by its higher ROC-AUC. To ensure robustness, we extended this comparison to two independent testing sets. Figure 5B shows the ROC-AUC values across the Liu cohort and both testing sets. Notably, iPRISM consistently achieved the highest AUC values in all datasets, indicating its reliability and effectiveness across diverse patient populations.

Beyond predictive accuracy, we evaluated the prognostic significance of iPRISM through univariate and multivariate Cox analysis. The univariate analysis (Figure 5C) compared the hazard ratios of various markers, including those from the TIDE framework,[20] to assess their individual prognostic value. iPRISM yielded the significantly highest hazard ratio, indicating its superior ability to provide critical prognostic features regarding patient survival.

To examine the independence and robustness of the predictive markers used in iPRISM, we conducted a multivariate Cox analysis (Figure 5D). This analysis aimed to determine whether the markers and features retain their predictive power when considered collectively. iPRISM outperformed all other methods, exhibiting the greatest hazard ratio and the highest statistical

© 2024 The Author(s). Advanced Intelligent Systems published by Wiley-VCH GmbH

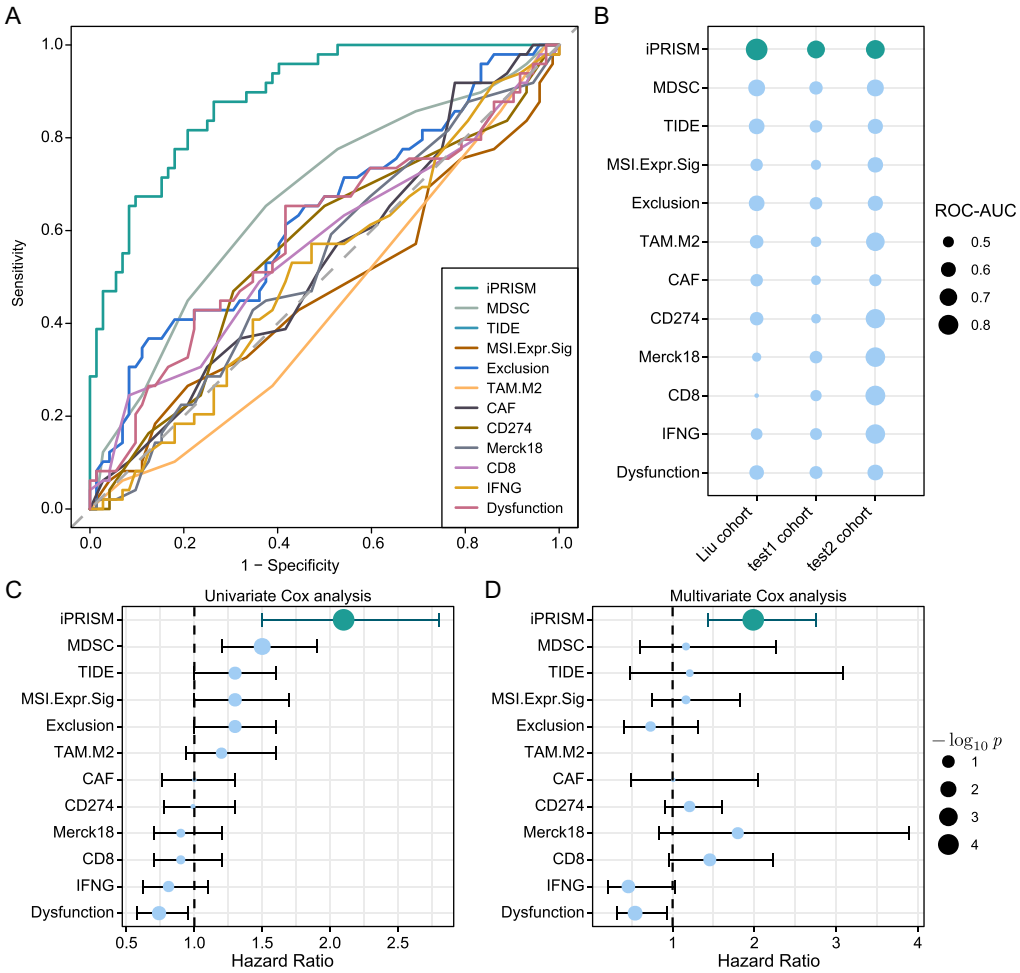

Figure 5. Comparative analysis of iPRISM with other methods. A) ROC curves comparing the iPRISM model with 11 other methods using the Liu cohort, demonstrating superior performance of iPRISM. B) Comparative ROC-AUC values for iPRISM and other methods across the Liu cohort and two independent testing sets, highlighting the robust performance of iPRISM. C) Univariate Cox analysis of various markers with 95% confidence interval, including those in TIDE framework, showing hazard ratios and indicating the iPRISM model's superior prognostic power. D) Multivariate Cox analysis assessing the independence of predictive markers with 95% confidence interval, with iPRISM model showing the lowest hazard ratio and highest statistical significance.

significance. This demonstrates that the predictive markers in iPRISM are robust and independent, further validating its prognostic utility in melanoma.

3.5. Application of the iPRISM Model to Other Cancer Types

To assess the generalizability and effectiveness of the iPRISM model beyond melanoma, we extended our validation to other cancer types, including BLCA, NSCLC, and STAD which are suitable for immunotherapy. This section of evaluation aimed to demonstrate its versatility across different cancer contexts.

In BLCA, we compared iPRISM with other methods to evaluate its predictive accuracy and prognostic significance. **Figure 6**A, B present the ROC curves, showing that iPRISM outperforms other methods with a higher ROC-AUC in IMvigor210 dataset (Figure 6A,B). Its classification ability was further validated using the chi-square test (Figure 6C), yielding a high significant p-value, which indicates a strong association between its prediction and actual immunotherapy responses. The survival analysis in Figure 6D demonstrates a significant difference in Kaplan–Meier curves between predicted responders and nonresponders ($p < 0.0001$), indicating the significant prognostic prediction power.

For NSCLC, iPRISM demonstrated superior performance compared to other methods, the ROC curves showed that iPRISM achieves the highest predictive accuracy across all methods evaluated in GSE93157 dataset (Figure 6E,F).[27] We assess its classification accuracy using a Chi-square test (Figure 6G). This test yielded a significant p-value ($p = 0.015$), confirming its effectiveness in classifying drug responses. The survival analysis in Figure 6H shows a significant difference in OS between predicted responders and nonresponders ($p = 0.035$), reinforcing the model's prognostic utility in NSCLC.

In STAD, we focused on the model's classification and prediction accuracy due to the absence of survival information in the dataset. We demonstrated the ROC curves in Figure S4A,

© 2024 The Author(s). Advanced Intelligent Systems published by Wiley-VCH GmbH

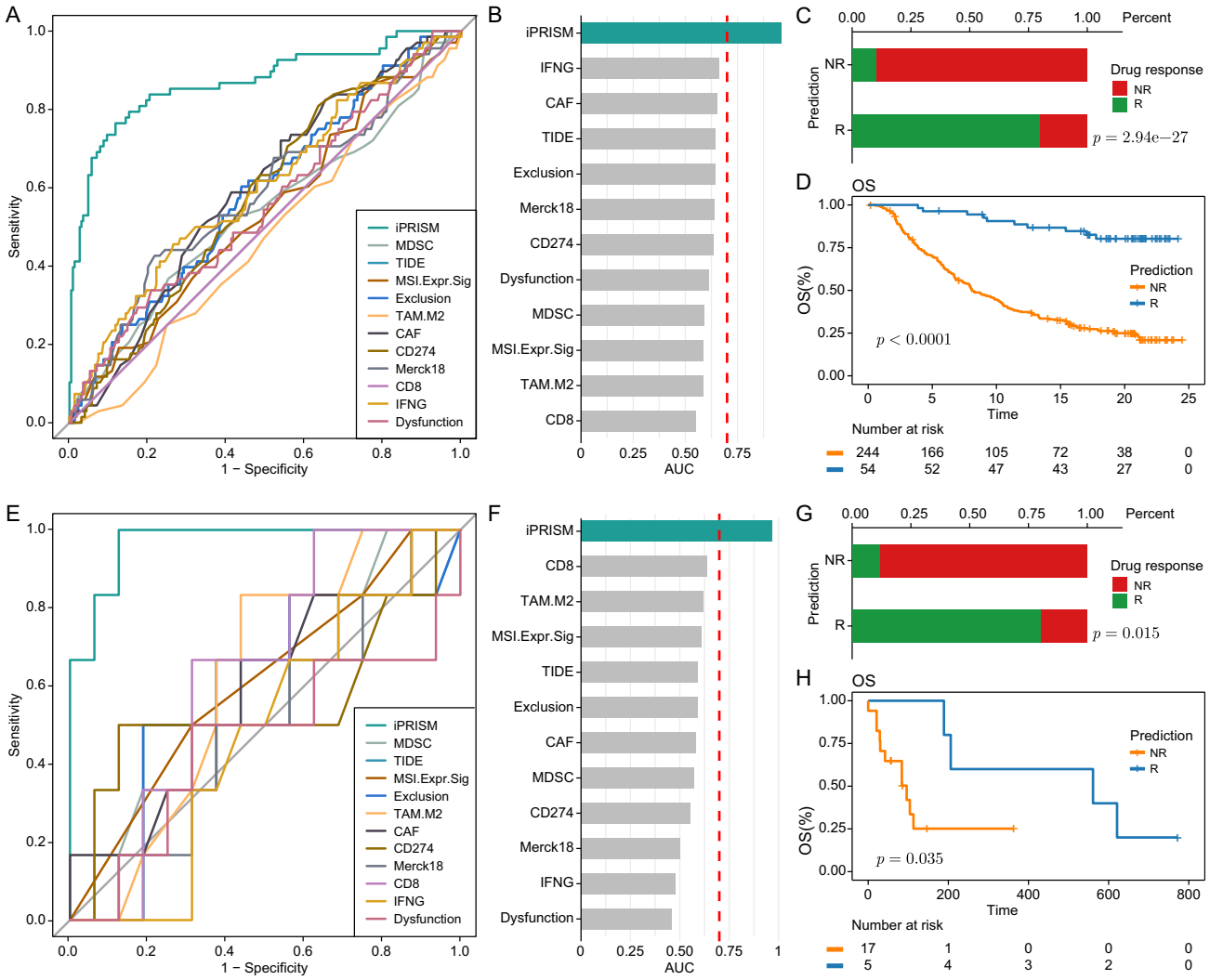

Figure 6. Validation of iPRISM in BLCA and NSCLC. A) ROC curves comparing iPRISM model with other methods in BLCA cohort, demonstrating its superior performance. B) Comparative ROC-AUC values in BLCA cohort, highlighting iPRISM model's high predictive accuracy. C) Chi-square test results showing significant association between the model predictions and actual drug responses in the BLCA cohort ($p = 2.94e\text{-}27$). D) Kaplan–Meier survival curves for OS in the BLCA cohort, showing a significant difference between predicted responders and nonresponders ($p < 0.0001$). E) ROC curves comparing iPRISM model with other methods in NSCLC cohort, demonstrating superior performance by the iPRISM model. F) Comparative ROC-AUC values in the NSCLC cohort, highlighting the model's high predictive accuracy. G) Chi-square test results showing significant association between the model predictions and actual drug responses in the NSCLC cohort ($p = 0.015$). H) Kaplan–Meier survival curves for OS in the NSCLC cohort, showing a significant difference between predicted responders and nonresponders ($p = 0.035$).

Supporting Information, and it shows the competitive performance against other methods in PRJEB25780 dataset.[28] Comparison of AUC values in Figure S4B, Supporting Information showed that iPRISM achieved one of the highest AUCs. The classification accuracy is significant (Figure S4C, Supporting Information), indicating a strong correlation between predictions and actual drug responses. These results underscore the iPRISM model's effectiveness in predicting treatment outcomes in STAD.

Overall, these evaluations across multiple cancer types demonstrate the versatility and robustness of iPRISM in predicting immunotherapy responses and patient outcomes beyond its original application in melanoma.

3.6. iPRISM Can Capture the Biological Mechanisms Underlying Immunotherapy Responses

Building upon our previous finding demonstrating the predictive and prognostic capabilities across multiple cancer types, we further applied this model to gain insights into the biological mechanisms involved in immunotherapy responses. Using Liu cohort, we applied iPRISM to gain insights into the TME differences between predicted responders and nonresponders.

According to **Figure 7**A, results in GSEA highlighted several pathways enriched in predicted responders and nonresponders. Among the top pathways identified, the Th1 and Th2 cell differentiation pathway emerged as a key factor. This finding

© 2024 The Author(s). Advanced Intelligent Systems published by Wiley-VCH GmbH

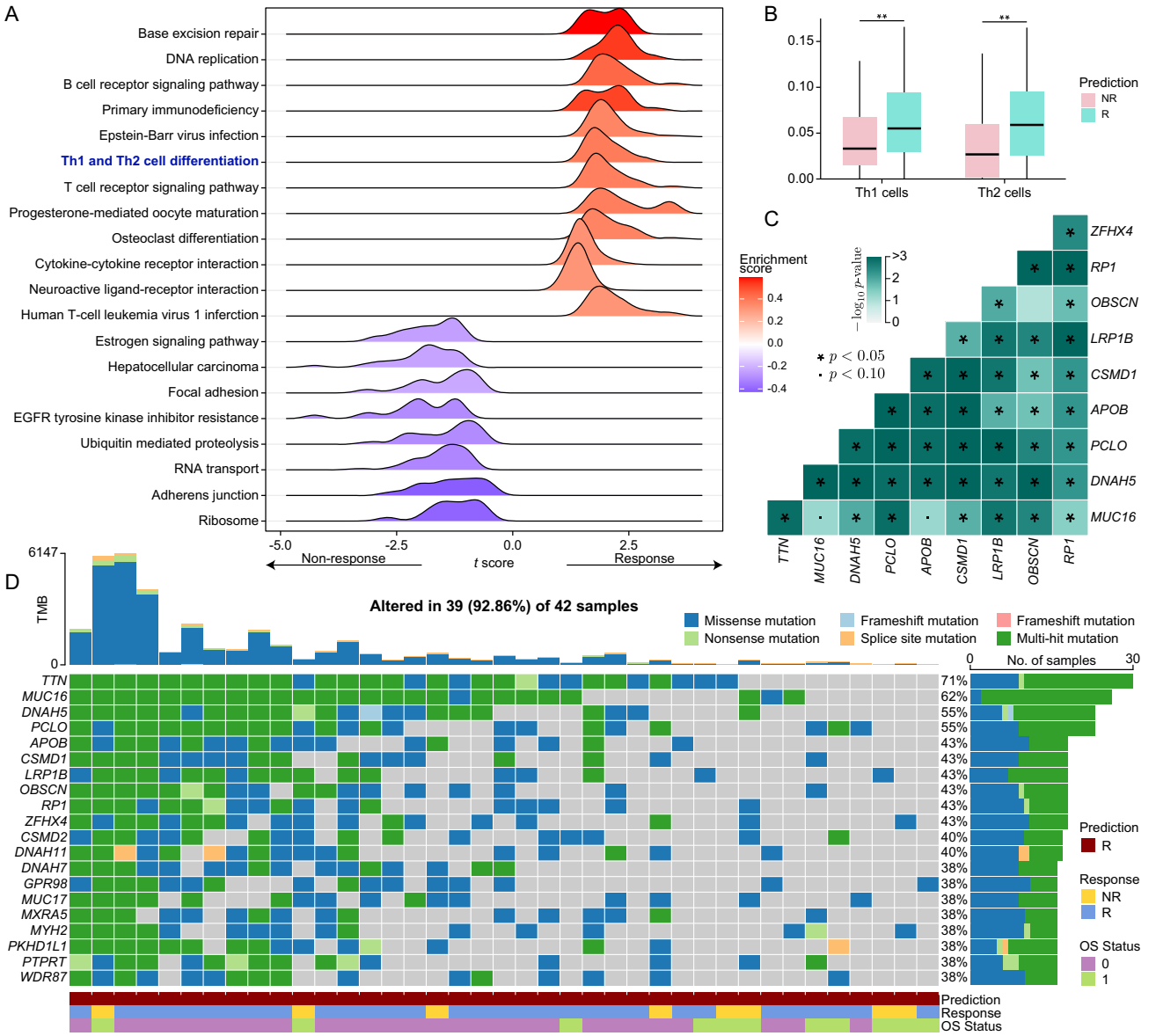

Figure 7. Further analysis of tumor immunotherapy mechanisms. A) GSEA enrichment results of core genes in the Liu cohort, arranged by pathway t-scores. Response-associated pathways are positioned to the right, with Th1 and Th2 cell differentiation pathway among the top pathways. B) Comparison of Th1 and Th2 cell infiltration levels between predicted responders and nonresponders using the xCell tool, showing significantly higher infiltration in responders. C) Analysis of top 10 genes with mutually exclusive or co-occurring mutations in responders. Color indicates p-values of mutually exclusive co-occurring; dots and asterisks represent correlation p-values. D) Waterfall plot depicting mutation distribution and frequency in patients predicted to be responders.

underscores the crucial role of these T helper cells in modulating immune responses against melanoma, potentially influencing the efficacy of immunotherapy. This pathway aligns with recent studies showing that Th1 cells play a pivotal role in antitumor immunity by activating cytotoxic T cells and natural killer cells through interferon gamma (IFN-γ) secretion, while Th2 cells can promote an immunosuppressive environment that may aid tumor growth through interleukin 4 (IL-4) production.[38] Quantitative analysis of Th1 and Th2 cell infiltration levels using xCell revealed significantly higher infiltration levels in responders ($p < 0.01$), as shown in Figure 7B, indicating a more robust antitumor immune response in responders. The association between higher Th1 and Th2 cell infiltration and positive responses to immunotherapy has been corroborated by findings that a balanced Th1/Th2 response is crucial for effective antitumor immunity, and a skew toward Th2 can facilitate tumor immune evasion.[39]

To understand the genetic landscape influencing these immune responses, we analyzed the model behind iPRISM to analyze mutation profiles in predicted responders and nonresponders. In predicted responders, we identified significant patterns of co-occurrence and mutually exclusivity among the top 10

© 2024 The Author(s). Advanced Intelligent Systems published by Wiley-VCH GmbH

mutated genes (Figure 7C). Notably, genes such as *TTN*, *MUC16*, and *DNAH5* showed exclusively relationships, suggesting potential synergistic interactions that may enhance antitumor immune responses. The waterfall plots (Figure 7D) reveal that 92.86% (39 out of 42) of predicted responders frequently harbored mutations in these key genes, providing a genetic signature that correlates with positive immunotherapy outcomes.

Conversely, predicted nonresponders exhibited distinct mutation profiles (Figure S5A, Supporting Information). In this group, 91.14% (72 out of 79) of samples frequently carried mutations in genes including *MUC16*, *BRAF*, and *CSMD1*. The co-occurrence and mutual exclusivity patterns in nonresponders (Figure S5B, Supporting Information) differed from those in responders, potentially contributing to mechanisms of immunotherapy resistance. For instance, *BRAF* mutations lead to the activation of the MAPK pathway, which is essential for immune evasion by human melanoma cells.[40] Similarly, the presence of mutations in *CSMD1*, a gene implicated in tumor suppression, suggests a loss of function that may further facilitate immune evasion and tumor progression.[41]

4. Discussion

Our study demonstrates the efficacy of the iPRISM model in predicting responses to immunotherapy across diverse cancer types. By integrating multiple types of biological data, including gene expression profiles and immune-related pathways, our approach offers a comprehensive framework for patient stratification and treatment planning, and replicates previous findings using the view of bioinformatics.

A primary strength of iPRISM lies in its comprehensive integration of existing biological data. By incorporating gene expression profiles, biological network, TME characteristics, immune-related pathways, and patient clinical outcomes, the iPRISM model provides a holistic view of factors influencing immunotherapy responses. The use of advanced feature selection techniques, such as GSEA and ssGSEA, ensures the inclusion of only the most relevant pathways and genes.[42] This is evidenced by the high AUC values and significant survival benefits observed in both training and independent testing cohorts. Furthermore, the stepwise logistic regression employed efficiently identifies the most relevant predictors from a large set of potential variables.[43]

Our analysis reveals a spectrum of mutations in nonresponders highlights key mechanisms of immunotherapy resistance. These mechanisms include immune evasion strategies and alterations in critical signaling pathways. Notably, mutations in the Wnt/β-catenin pathway have been associated with immune exclusion by creating a "cold" tumor microenvironment that is less infiltrated by immune cells.[44] This pathway prevents the effective activation and recruitment of cytotoxic T cells, thereby diminishing immunotherapy efficacy.

Immune evasion presents an extensive challenge in cancer immunotherapy. Tumors can evade immune detection through various strategies, including the production of immunosuppressive factors like transforming growth factor beta (TGF-β) and the recruitment of immunosuppressive cells such as tumor-associated macrophages and myeloid-derived suppressor cells.[45–47] Additionally, tumors may lose neoantigens or develop impairments in antigen processing and presentation machinery,[48,49] such as mutations in β-2-microglobulin and HLA molecules.[48] These factors and alterations in signaling pathways such as *PTEN* loss, along with upregulation of immunosuppressive cytokines such as TGF-β, collectively contribute to the resistance observed in nonresponders by creating an environment that excludes cytotoxic T cells and supports tumor growth.[50]

The iPRISM model builds upon and enhances previous studies in immunotherapy prediction. While it confirms the importance of immune-related pathways identified in earlier studies, it also provides novel insights through its comprehensive data integration. Our findings emphasize the crucial role of comprehensive molecular profiling in understanding and surmounting immunotherapy resistance. The enrichment of Th1 and Th2 cell differentiation pathways among responders highlights the critical role of these immune cells in mediating effective antitumor responses.[51] Higher infiltration levels of Th1 and Th2 cells in responders suggest their crucial role in determining immunotherapy outcomes.

The ability to accurately predict immunotherapy responses and provide prognostic insights of iPRISM has significant clinical implications. By identifying key genetic and signaling alterations, we can develop targeted therapies to inhibit specific resistance mechanisms.[52] For example, combining immune checkpoint inhibitors with therapies targeting the Wnt/β-catenin pathway or TGF-β signaling may enhance the efficacy of immunotherapy.[53] Moreover, strategies to modulate the tumor microenvironment, such as nanomedicine-based approaches to reverse immunosuppression, offer promising insights for improving treatment outcomes.[54]

While iPRISM demonstrates considerable strengths, it is essential to acknowledge its potential limitations. One such limitation is the dependence on the quality and completeness of input data. Although iPRISM is trained and validated from various cohorts, variations in data acquisition methods and preprocessing techniques could introduce noise and bias. These variations could affect its performance across different patient populations and lab environments. To address this, incorporating more diverse datasets would improve the robustness and allow for broader application in clinical settings.

Furthermore, the model relies on static gene expression and mutation data collected at baseline, which may not capture all the characteristics of the TME and immune response over the course of the treatment. As patients receiving treatment, changes in the TME could alter the response to treatment. Incorporating longitudinal data into iPRISM would allow for more accurate estimates of long-term outcomes, which further provide more personalized treatment recommendations.

We have wrapped the core functions to an R package. Researchers can adjust the number of pathways by modifying significance thresholds to broaden or narrow down the analysis. To our concerns, retaining fewer, highly significant pathways can result in a simpler model, which may generalize better and reduce the risk of overfitting. Conversely, including more features can increase model complexity, which may improve prediction accuracy. Additionally, researchers can incorporate other

© 2024 The Author(s). Advanced Intelligent Systems published by Wiley-VCH GmbH

pathways based on other well-established databases rather than Reactome, such as Kyoto Encyclopedia of Genes and Genomes (KEGG) or GO. In this case, researchers can include pathways beyond the immune-related initially identified in iPRISM, which can enable researchers to explore specific questions or hypotheses according to their needs.

In conclusion, iPRISM represents a robust and reproducible tool for predicting immunotherapy responses and providing prognostic insights across multiple cancer types. Its integration of diverse biological relevance highlights its potential for guiding personalized treatment strategies. Future research should focus on adaptive treatment strategies to dynamically counteract resistance mechanisms. The use of combination therapies, personalized to the mutational and immunological profile of each patient, holds great promise in improving the efficacy of immunotherapy.[55] By addressing the underlying mechanisms of resistance, our approach paves the way for more effective and tailored treatment strategies, ultimately improving clinical outcomes for cancer patients.

Supporting Information

Supporting Information is available from the Wiley Online Library or from the author.

Acknowledgements

During the preparation of this manuscript and the documentation of the labyrinth, the authors employed Claude for grammatical corrections and enhancements in readability. The authors thoroughly reviewed and took great care of the content to ensure its quality, making edits as necessary. Consequently, the authors take full responsibility for the content presented in this work. This work was supported by the National Natural Science Foundation of China (grant nos. 62372 143 and 62072 145) and the Natural Science Foundation of Heilongjiang Province (grant no. LH2019C042).

Conflict of Interest

The authors declare no conflict of interest.

Author Contributions

Yinchun Su: data curation (equal); formal analysis (equal); investigation (equal); methodology (equal); software (equal); visualization (equal); writing—original draft (equal). **Siyuan Li**: data curation (equal); formal analysis (equal); investigation (equal); visualization (equal); writing—review and editing (equal). **Qian Wang**: data curation (equal); formal analysis (equal); investigation (equal); methodology (equal); software (equal); visualization (equal); writing—review and editing (equal). **Bingyue Pan**: data curation (equal); formal analysis (equal); investigation (equal); validation (equal). **Jiyin Lai**: data curation (equal); formal analysis (equal); investigation (equal). **Guangyou Wang**: supervision (equal). **Junwei Han**: conceptualization (equal); funding acquisition (equal); project administration (equal); supervision (equal); writing—original draft (equal). **Qingfei Kong**: conceptualization (equal); supervision (equal); writing—original draft (equal). **Yinchun Su**, **Siyuan Li**, and **Qian Wang**: contributed equally to this work.

Data Availability Statement

The datasets utilized in this study are publicly available. The Liu cohort is available from the study by Liu et al. and can be assessed in cBioPortal (https://www.cbioportal.org/study/summary?id=mel_dfci_2019). For independent validation, we employed two testing sets: PRJEB23709 and phs000452, both of which can be accessed through the TIGER portal at http://tiger.canceromics.org/#/download. Additionally, we used IMvigor210 dataset for BLCA analysis, which is available through the IMvigor210CoreBiologies R package on GitHub (https://github.com/SiYangming/IMvigor210CoreBiologies). The NSCLC dataset (GSE93157) can be obtained from the Gene Expression Omnibus (GEO) repository. The STAD dataset (PRJEB25780) is also accessible via the TIGER portal.

Code Availability Statement

We have wrapped the core function into an R package named iPRISM (Intelligent Predicting Response to cancer Immunotherapy through Systematic Modeling), which is freely available under the GPL-v2 license at CRAN (https://CRAN.R-project.org/package=iPRISM). To specify, iPRISM can be effectively run on low-budget hardware. We retrained iPRISM model using our R package in the low-end single-core environment and consumes about six hours and four gigabytes of memory in this instance.

Keywords

immunotherapy, network-based models, pathway analysis, personalized medicine, prognostic signature

Received: August 20, 2024
Revised: October 31, 2024
Published online:

[1] I. O. Okoduwa, B. I. Ashiwaju, J. O. Ogugua, J. O. Arowoogun, K. F. Awonuga, E. C. Anyanwu, *World J. Biol. Pharm. Health Sci.* **2024**, *17*, 068.
[2] K. M. Hargadon, C. E. Johnson, C. J. Williams, *Int. Immunopharmacol.* **2018**, *62*, 29.
[3] C. M. Fares, E. M. Van Allen, C. G. Drake, J. P. Allison, S. Hu-Lieskovan, *Am. Soc. Clin. Oncol. Educ. Book* **2019**, *39*, 147.
[4] R. Bai, N. Chen, L. Li, N. Du, L. Bai, Z. Lv, H. Tian, J. Cui, *Front. Oncol.* **2020**, *10*, 1290.
[5] C. Pilard, M. Ancion, P. Delvenne, G. Jerusalem, P. Hubert, M. Herfs, *Br. J. Cancer* **2021**, *125*, 927.
[6] N. D. Shore, *BJU Int.* **2015**, *116*, 321.
[7] F. Galli, J. V. Aguilera, B. Palermo, S. N. Markovic, P. Nisticò, A. Signore, *J. Exp. Clin. Cancer Res.* **2020**, *39*, 89.
[8] O. A. W. Haabeth, K. B. Lorvik, C. Hammarström, I. M. Donaldson, G. Haraldsen, B. Bogen, A. Corthay, *Nat. Commun.* **2011**, *2*, 240.
[9] K. B. Lorvik, C. Hammarström, M. Fauskanger, O. A. W. Haabeth, M. Zangani, G. Haraldsen, B. Bogen, A. Corthay, *Cancer Res.* **2016**, *76*, 6864.
[10] Y.-T. Liu, Z.-J. Sun, *Theranostics* **2021**, *11*, 5365.
[11] D. Cao, H. Xu, X. Xu, T. Guo, W. Ge, *OncoImmunology* **2019**, *8*, e1629258.
[12] N. A. Rizvi, M. D. Hellmann, A. Snyder, P. Kvistborg, V. Makarov, J. J. Havel, W. Lee, J. Yuan, P. Wong, T. S. Ho, M. L. Miller, N. Rekhtman, A. L. Moreira, F. Ibrahim, C. Bruggeman, B. Gasmi, R. Zappasodi, Y. Maeda, C. Sander, E. B. Garon, T. Merghoub, J. D. Wolchok, T. N. Schumacher, T. A. Chan, *Science* **2015**, *348*, 124.

© 2024 The Author(s). Advanced Intelligent Systems published by Wiley-VCH GmbH

[13] S. J. Patel, N. E. Sanjana, R. J. Kishton, A. Eidizadeh, S. K. Vodnala, M. Cam, J. J. Gartner, L. Jia, S. M. Steinberg, T. N. Yamamoto, A. S. Merchant, G. U. Mehta, A. Chichura, O. Shalem, E. Tran, R. Eil, M. Sukumar, E. P. Guijarro, C.-P. Day, P. Robbins, S. Feldman, G. Merlino, F. Zhang, N. P. Restifo, *Nature* **2017**, *548*, 537.
[14] R. M. Samstein, C.-H. Lee, A. N. Shoushtari, M. D. Hellmann, R. Shen, Y. Y. Janjigian, D. A. Barron, A. Zehir, E. J. Jordan, A. Omuro, T. J. Kaley, S. M. Kendall, R. J. Motzer, A. A. Hakimi, M. H. Voss, P. Russo, J. Rosenberg, G. Iyer, B. H. Bochner, D. F. Bajorin, H. A. Al-Ahmadie, J. E. Chaft, C. M. Rudin, G. J. Riely, S. Baxi, A. L. Ho, R. J. Wong, D. G. Pfister, J. D. Wolchok, C. A. Barker, et al., *Nat. Genet.* **2019**, *51*, 202.
[15] A. M. Goodman, S. Kato, L. Bazhenova, S. P. Patel, G. M. Frampton, V. Miller, P. J. Stephens, G. A. Daniels, R. Kurzrock, *Mol. Cancer Ther.* **2017**, *16*, 2598.
[16] Y. Wu, J. Xu, C. Du, Y. Wu, D. Xia, W. Lv, J. Hu, *Front. Oncol.* **2019**, *9*, 1161.
[17] S. Liu, S. Geng, N. Shi, L. Zhang, W. Xue, Y. Li, K. Jiang, *Front. Pharmacol.* **2022**, *13*, 878540.
[18] W. D. Roock, V. D. Vriendt, N. Normanno, F. Ciardiello, S. Tejpar, *Lancet Oncol.* **2011**, *12*, 594.
[19] D. Marinelli, M. Mazzotta, S. Scalera, I. Terrenato, F. Sperati, L. D'Ambrosio, M. Pallocca, G. Corleone, E. Krasniqi, L. Pizzuti, M. Barba, S. Carpano, P. Vici, M. Filetti, R. Giusti, A. Vecchione, M. Occhipinti, A. Gelibter, A. Botticelli, F. De Nicola, L. Ciuffreda, F. Goeman, E. Gallo, P. Visca, E. Pescarmona, M. Fanciulli, R. De Maria, P. Marchetti, G. Ciliberto, M. Maugeri-Saccà, *Ann. Oncol.* **2020**, *31*, 1746.
[20] P. Jiang, S. Gu, D. Pan, J. Fu, A. Sahu, X. Hu, Z. Li, N. Traugh, X. Bu, B. Li, J. Liu, G. J. Freeman, M. A. Brown, K. W. Wucherpfennig, X. S. Liu, *Nat. Med.* **2018**, *24*, 1550.
[21] T. J. Nielsen, B. Z. Ring, R. S. Seitz, D. R. Hout, B. L. Schweitzer, *Heliyon* **2021**, *7*, e06438.
[22] Z.-Y. Qian, Y.-Q. Pan, X.-X. Li, Y.-X. Chen, H.-X. Wu, Z.-X. Liu, M. Kosar, J. Bartek, Z.-X. Wang, R.-H. Xu, *Sci. Bull.* **2024**, *69*, 803.
[23] D. Liu, B. Schilling, D. Liu, A. Sucker, E. Livingstone, L. Jerby-Arnon, L. Zimmer, R. Gutzmer, I. Satzger, C. Loquai, S. Grabbe, N. Vokes, C. A. Margolis, J. Conway, M. X. He, H. Elmarakeby, F. Dietlein, D. Miao, A. Tracy, H. Gogas, S. M. Goldinger, J. Utikal, C. U. Blank, R. Rauschenberg, D. von Bubnoff, A. Krackhardt, B. Weide, S. Haferkamp, F. Kiecker, B. Izar, et al., *Nat. Med.* **2019**, *25*, 1916.
[24] T. N. Gide, C. Quek, A. M. Menzies, A. T. Tasker, P. Shang, J. Holst, J. Madore, S. Y. Lim, R. Velickovic, M. Wongchenko, Y. Yan, S. Lo, M. S. Carlino, A. Guminski, R. P. M. Saw, A. Pang, H. M. McGuire, U. Palendira, J. F. Thompson, H. Rizos, I. P. da Silva, M. Batten, R. A. Scolyer, G. V. Long, J. S. Wilmott, *Cancer Cell* **2019**, *35*, 238.
[25] E. M. Van Allen, D. Miao, B. Schilling, S. A. Shukla, C. Blank, L. Zimmer, A. Sucker, U. Hillen, M. H. G. Foppen, S. M. Goldinger, J. Utikal, J. C. Hassel, B. Weide, K. C. Kaehler, C. Loquai, P. Mohr, R. Gutzmer, R. Dummer, S. Gabriel, C. J. Wu, D. Schadendorf, L. A. Garraway, *Science* **2015**, *350*, 207.
[26] S. Mariathasan, S. J. Turley, D. Nickles, A. Castiglioni, K. Yuen, Y. Wang, E. E. Kadel Iii, H. Koeppen, J. L. Astarita, R. Cubas, S. Jhunjhunwala, R. Banchereau, Y. Yang, Y. Guan, C. Chalouni, J. Ziai, Y. Şenbabaoğlu, S. Santoro, D. Sheinson, J. Hung, J. M. Giltnane, A. A. Pierce, K. Mesh, S. Lianoglou, J. Riegler, R. A. D. Carano, P. Eriksson, M. Höglund, L. Somarriba, D. L. Halligan, et al., *Nature* **2018**, *554*, 544.
[27] A. Prat, A. Navarro, L. Paré, N. Reguart, P. Galván, T. Pascual, A. Martínez, P. Nuciforo, L. Comerma, L. Alos, N. Pardo, S. Cedrés, C. Fan, J. S. Parker, L. Gaba, I. Victoria, N. Viñolas, A. Vivancos, A. Arance, E. Felip, *Cancer Res.* **2017**, *77*, 3540.
[28] S. T. Kim, R. Cristescu, A. J. Bass, K.-M. Kim, J. I. Odegaard, K. Kim, X. Q. Liu, X. Sher, H. Jung, M. Lee, S. Lee, S. H. Park, J. O. Park, Y. S. Park, H. Y. Lim, H. Lee, M. Choi, A. Talasaz, P. S. Kang, J. Cheng, A. Loboda, J. Lee, W. K. Kang, *Nat. Med.* **2018**, *24*, 1449.
[29] D. Aran, Z. Hu, A. J. Butte, *Genome Biol.* **2017**, *18*, 220.
[30] A. Mayakonda, D.-C. Lin, Y. Assenov, C. Plass, H. P. Koeffler, *Genome Res.* **2018**, *28*, 1747.
[31] X. Wang, A. M. Bove, G. Simone, B. Ma, *Front. Cell Dev. Biol.* **2020**, *8*, 599281.
[32] A. Sadremomtaz, K. Mansouri, G. Alemzadeh, M. Safa, A. E. Rastaghi, S. M. Asghari, *Biochim. Biophys. Acta BBA - Gen. Sub.* **2018**, *1862*, 2688.
[33] E. R. Asl, M. Amini, S. Najafi, B. Mansoori, A. Mokhtarzadeh, A. Mohammadi, P. Lotfinejad, M. Bagheri, S. Shirjang, Z. Lotfi, Y. Rasmi, B. Baradaran, *Life Sci.* **2021**, *278*, 119499.
[34] B. L. Jakubison, T. Sarkar, K. O. Gudmundsson, S. Singh, L. Sun, H. M. Morris, K. D. Klarmann, J. R. Keller, *J. Clin. Invest.* **2022**, *132*, e152599.
[35] B. Ling, Y. Xu, S. Qian, Z. Xiang, S. Xuan, J. Wu, *Front. Cell Dev. Biol.* **2023**, *11*, 1186850.
[36] C. D. Wiley, M. C. Velarde, P. Lecot, S. Liu, E. A. Sarnoski, A. Freund, K. Shirakawa, H. W. Lim, S. S. Davis, A. Ramanathan, A. A. Gerencser, E. Verdin, J. Campisi, *Cell Metab.* **2016**, *23*, 303.
[37] Y. Ueda, D. W. Cain, M. Kuraoka, M. Kondo, G. Kelsoe, *J. Immunol.* **2009**, *182*, 6477.
[38] A. Basu, G. Ramamoorthi, G. Albert, C. Gallen, A. Beyer, C. Snyder, G. Koski, M. L. Disis, B. J. Czerniecki, K. Kodumudi, *Front. Immunol.* **2021**, *12*, 669474.
[39] Y. Qiu, T. Chen, R. Hu, R. Zhu, C. Li, Y. Ruan, X. Xie, Y. Li, *Biomarker Res.* **2021**, *9*, 72.
[40] H. Sumimoto, F. Imabayashi, T. Iwata, Y. Kawakami, *J. Exp. Med.* **2006**, *203*, 1651.
[41] H. Zhang, T. Huang, X. Ren, X. Fang, X. Chen, H. Wei, W. Sun, Y. Wang, *Front. Genet.* **2022**, *13*, 918486.
[42] A. Zito, M. Lualdi, P. Granata, D. Cocciadiferro, A. Novelli, T. Alberio, R. Casalone, M. Fasano, *Front. Genet.* **2021**, *12*, 577623.
[43] J.-S. Hwang, T.-H. Hu, *J. Stat. Comput. Simul.* **2015**, *85*, 1793.
[44] A. M. G. Wong, A. M. G. Wong, L. K. Can, J. Kwong, A. W. Chan, J. Chen, M. Kahn, N. Wong, *Cancer Res.* **2023**, *83*, 2886.
[45] E. Batlle, J. Massagué, *Immunity* **2019**, *50*, 924.
[46] M. Haist, H. Stege, S. Grabbe, M. Bros, *Cancers* **2021**, *13*, 210.
[47] S. Kusmartsev, D. I. Gabrilovich, *Cancer Immunol. Immunother.* **2006**, *55*, 237.
[48] S. Jhunjhunwala, C. Hammer, L. Delamarre, *Nat. Rev. Cancer* **2021**, *21*, 298.
[49] S. Peng, S. Chen, W. Hu, J. Mei, X. Zeng, T. Su, W. Wang, Z. Chen, H. Xiao, Q. Zhou, B. Li, Y. Xie, H. Hu, M. He, Y. Han, L. Tang, Y. Ma, X. Li, X. Zhou, Z. Dai, Z. Liu, J. Tan, L. Xu, S. Li, S. Shen, D. Li, J. Lai, B. Peng, Z. Peng, M. Kuang, *Cancer Immunol. Res.* **2022**, *10*, 728.
[50] S. H. Vu, P. Vetrivel, J. Kim, M.-S. Lee, *Int. J. Mol. Sci.* **2022**, *23*, 10906.
[51] K. L. Knutson, M. L. Disis, *Cancer Immunol. Immunother.* **2005**, *54*, 721.
[52] G. Tortora, R. Bianco, G. Daniele, F. Ciardiello, J. A. McCubrey, M. R. Ricciardi, L. Ciuffreda, F. Cognetti, A. Tafuri, M. Milella, *Drug Resist. Updates* **2007**, *10*, 81.
[53] S. Ganesh, X. Shui, K. P. Craig, J. Park, W. Wang, B. D. Brown, M. T. Abrams, *Mol. Ther.* **2018**, *26*, 2567.
[54] J. D. Martin, H. Cabral, T. Stylianopoulos, R. K. Jain, *Nat. Rev. Clin. Oncol.* **2020**, *17*, 251.
[55] R. Mandal, T. A. Chan, *Cancer Discovery* **2016**, *6*, 703.

© 2024 The Author(s). Advanced Intelligent Systems published by Wiley-VCH GmbH